JOURNAL OF MATERIALS SCIENCE 28 (1993) 5065–5069

Laser soldering of surface-mounted devices for high-reliability applications

E. SEMERAD
Department of Materials Technology, Austrian Research Center Seibersdorf, A-2444 Seibersdorf, Austria

L. MUSIEJOVSKY, J. NICOLICS
Institute of Materials for Electrical Engineering, Technical University Vienna, A-1040 Vienna, Austria

Laser soldering processes are characterized by the temperature during soldering within the joint as a function of time and as a function of the soldering parameters. These parameters are optimized by a metallurgical assessment of the quality of the joints. The thermal-fatigue properties of soldered joints important for space applications were investigated for different solder alloys by the thermal-cycling test according to ESA PSS-01-704. In addition, measurements of the shear strength were carried out for a small number of specimens in order to check if the mechanical strength of joints is altered by thermal cycling.

1. Introduction

With increasing miniaturization of electronic circuits, the demands of soldering technology have changed: printed circuit boards with through-hole components in industrial mass production are still wave soldered. For surface-mounted devices (SMDs), however, reflow technologies are frequently employed because of the sensitivity of the components to thermal shock and because of the risk of solder bridging due to their small spaced leads. Reflow techniques range from integral methods such as hot belt, infrared-radiation reflow, hot-gas reflow and vapour phase to single-joint-soldering methods like hot-bar reflow and last but not least laser soldering [1–5]. Single-soldering techniques can reach the heat levels of each solder joint individually. In this way, both high-quality solder joints are achievable and temperature-sensitive components can be reliably soldered.

2. Experimental procedure

In the present work the soldering pastes listed in Table I were compared. SO16 components with Cu and FeNi leads were soldered on FR4 printed circuit boards (PCBs). For the soldering a Nd–YAG continuous wave laser (multimode, focus diameter 1.2 mm) was used. The optimal parameter settings were determined by a series of soldering processes, whereby the laser power and the shutter-open interval (in the pulse duration) were varied systematically. In order to evaluate the solder-joint quality achieved, metallographic inspection and temperature measurements were carried out. A mere optical inspection of the components with the partially concealed solder joints was found to be insufficient to classify the solder-joint quality.

3. Results and discussion

3.1. Temperature measurement within a solder joint during soldering

For the analysis of the temperature change during the soldering process [6] solder joints with a 50 μm thick nickel-wire crossing a copper pad were prepared. These nickel-wires form thermocouples with the copper pads (Fig. 1). With this set up the temperature within the solder in the proximity of the copper pad is measured. Thus the temperature of the lead which is exposed to the laser radiation can assume higher values. On applying a laser pulse with 0.1 s duration

TABLE I Solder pastes

Solder type	Composition			Solidus temp. (°C)	Liquidus temp. (°C)	Supplier's metal content (%)	
	Sn	Pb	Ag				
Sn62	62	36	2	179	179	Demetron	89
Sn63	63	37		183	183	Demetron	90
Sn96	96.3		3.7	221	221	Multicore Sn96P-RMA-B5	75

0022–2461 © *1993 Chapman & Hall*

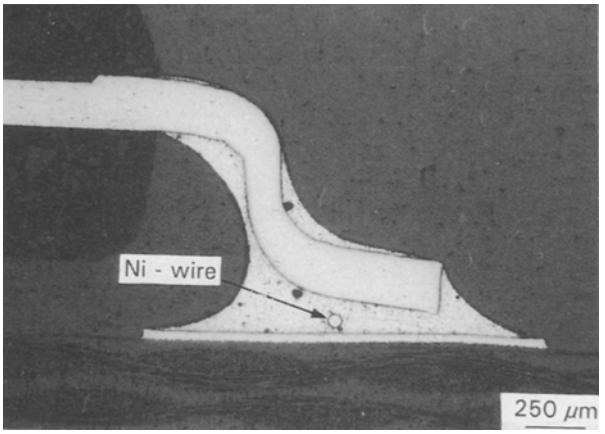

Figure 1 Cross-section of a solder joint, which is prepared for the measurement of temperature changes by means of a thermocouple consisting of a copper pad and a nickel wire of 50 μm diameter.

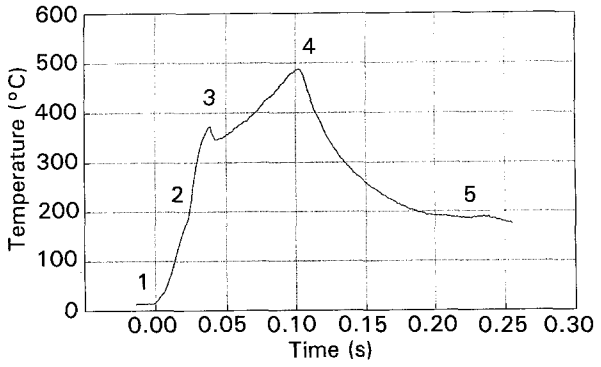

Figure 2 Temperature course measured in the solder joint shown in Fig. 1. Typical phases of the soldering process: (1–4) duration of the laser pulse, (2–3) melting of the solder, wetting of the lead, (3–4) wetting of the copper pad, and (5) recrystallization of the solder. Laser parameters: 20 W, 100 ms.

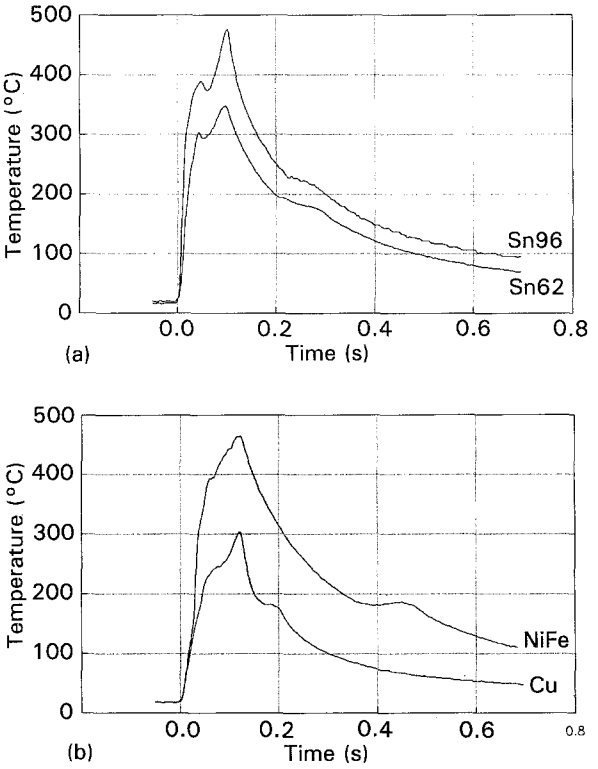

Figure 3 Comparison of temperature courses. Laser parameters: 20 W, 100 ms. (a) FeNi-leads, comparison of two different solders: Sn62 (melting point 179 °C) and Sn96 (melting point 221 °C). (b) Sn62 solder, comparison of two different lead materials: FeNi and Cu.

and a power of 20 W to form a solder joint between a copper lead of a SO-16 component and a copper pad on the FR-4 base material the temperature course shown in Fig. 2 typically appears. After opening the laser shutter (point 1) the temperature rises rapidly. Frequently a kink appears at the liquidus point (point 2); this is because the thermal conductivity of the already partially liquified solder is higher than that of the solder paste. In the next phase there is a sudden improvement in heat dissipation caused by the wetting of the solder pad; this sometimes causes a short temperature decrease (point 3) or at least a reduction in the rate of temperature increase. With the heat dissipation, the wetted area expands and the heat flow into the base material increases due to improved thermal contact between the solder and the copper pad. As a result of this, and because of the high reflectance of the completely molten solder, the further temperature rise is less strong than before. After closing the shutter (point 4), very high cooling rates–starting around 10^4 K s^{-1} for copper leads and 4×10^3 K s^{-1} for FeNi-leads, respectively–are obtained. This high rate is caused by the high heat dissipation into the component and into the base material, which remains at room temperature during soldering. On reaching the liquidus/solidus line (point 5) the solder crystallizes. After 100 ms the temperature decreases to a value below 100 °C.

The influence of different solders on the temperature course is presented in Fig. 3a. Because of the equal thermal time constants of the components, the various phases of the soldering process have the same length, but occur at different temperatures because of the unequal melting points of the solders. Therefore, they can be distinguished by the temperature during the period of crystallization. In Fig. 3b two temperatures courses, measured during soldering of FeNi-leads and copper leads with the same solder and the same laser parameters (18 W, 100 ms), are compared. As mentioned above, the different quantity of heat needed for producing these solder joints leads to different temperature courses after applying the same laser power. For the copper leads the chosen laser power is just sufficient, but for FeNi-leads it leads to burned remainders of flux. Also, different cooling rates can be observed clearly. Due to the higher thermal conductivity of the copper leads, the cooling rate is found to be 2.5 times as large as the rate for the FeNi-leads.

3.2. Metallographic assessment of the solder-joint quality

The solder fillets were examined under an optical microscope at a magnification of 50 times prior to the metallographical inspection. Cross-sections of joints of SO16 components with copper leads soldered with

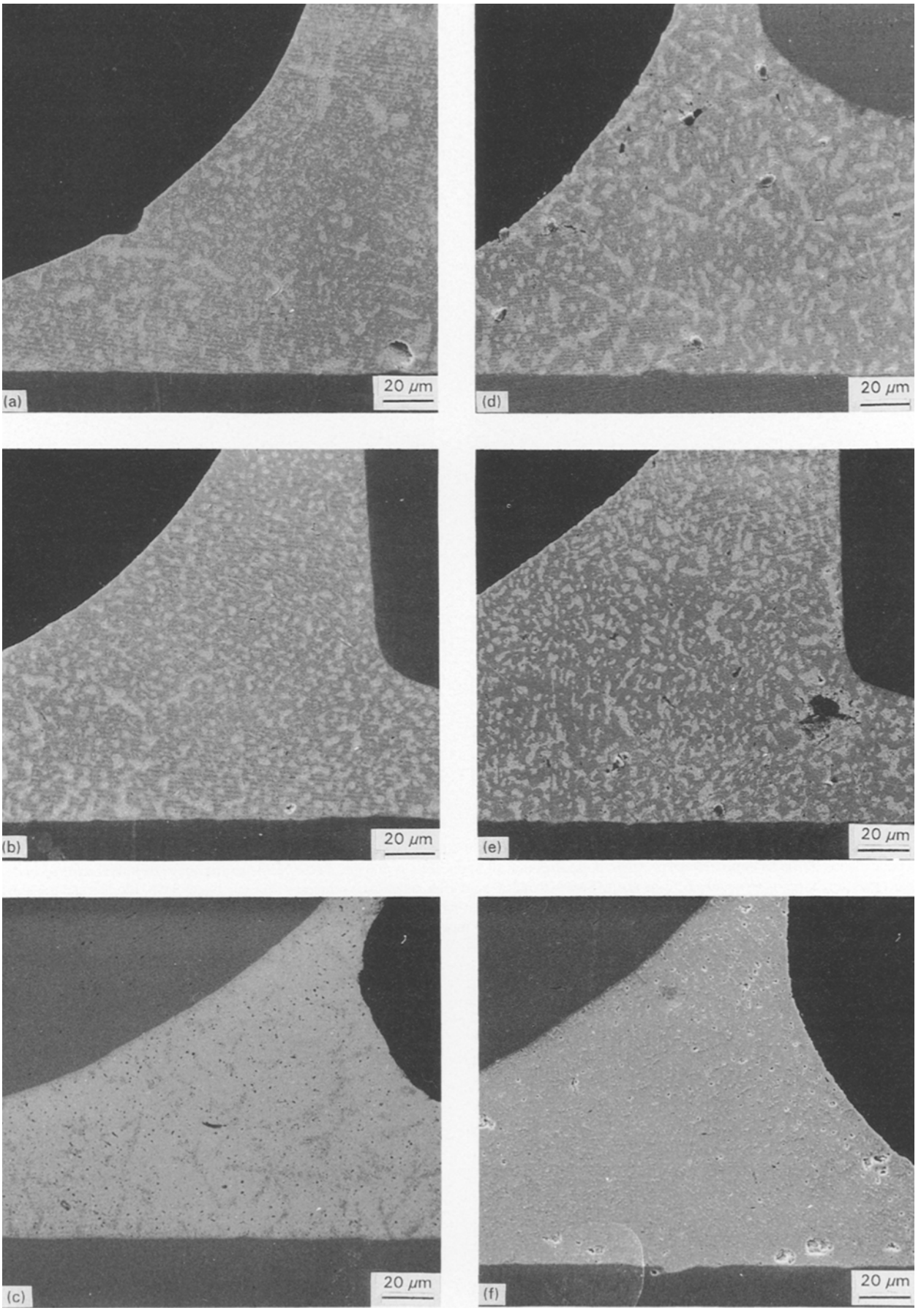

Figure 4 Secondary-electron-image SEM micrographs of the solder-joint microstructures for SO16 components with copper leads (laser power: 20 W for Sn62 and Sn63, 25 W for Sn96, pulse duration: 100 ms). (a) Sn62, uncycled; (b) Sn63, uncycled; (c) Sn96, uncycled; (d) Sn62, 100 thermal cycles; (e) Sn63, 100 thermal cycles; and (f) Sn96, 100 thermal cycles;

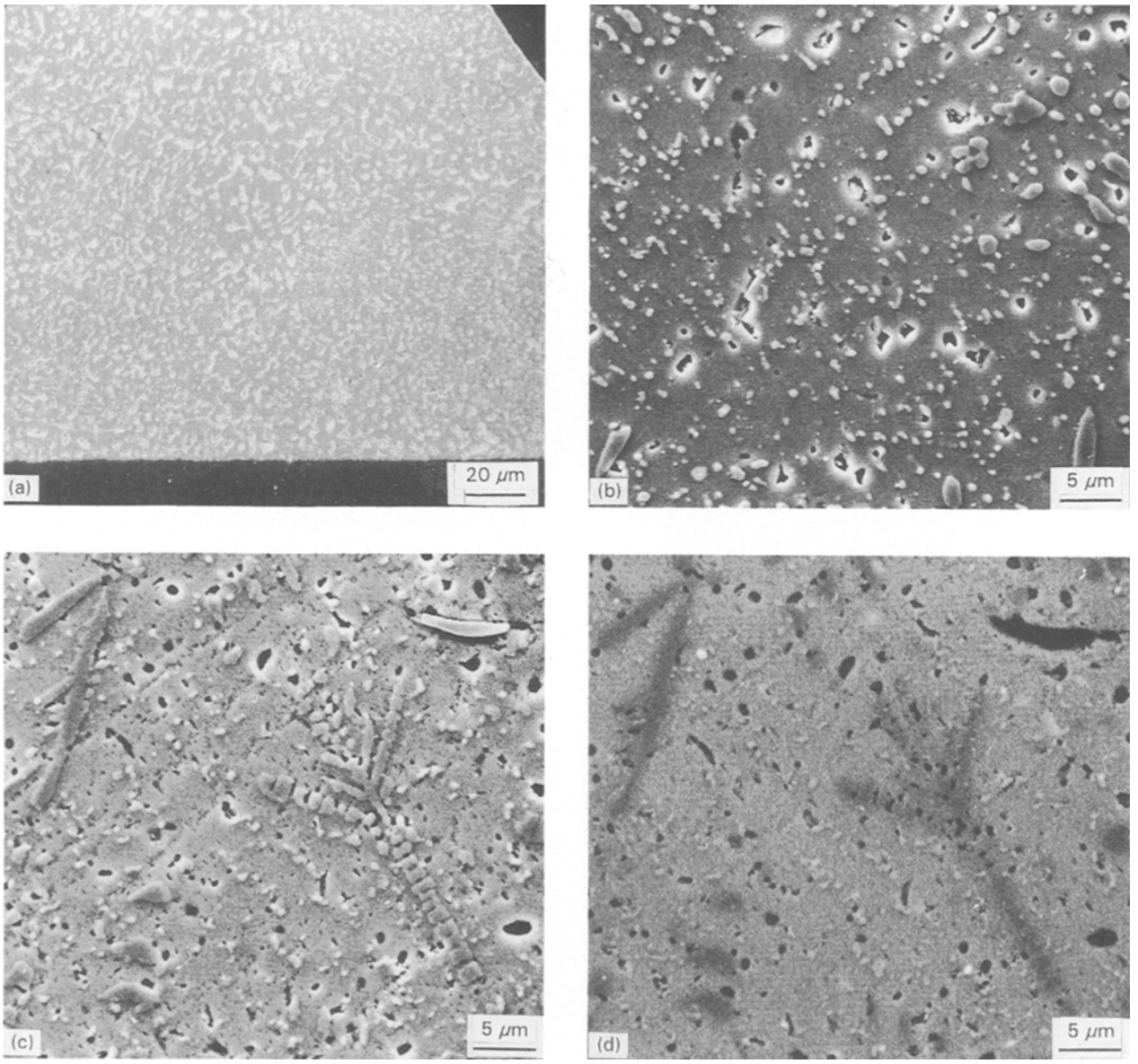

Figure 5 Solder-joint microstructures The details are in addition to Fig. 4, for SO16 components with copper leads. Laser power (if applicable) is 20 W for Sn63, 25 W for Sn96, pulse duration (if applicable) is 100 ms. These SEM micrographs are taken with secondary electrons (a), (b), (c) or reflected electrons (d). (a) Sn63, IR-reflow soldering, uncycled (compare with Fig. 4b); (b) Sn96, 100 thermal cycles (the magnification is higher than Fig. 4f to show details of the fine structure); (c) and (d) Sn96, uncycled (the dendrite structure is at higher magnification and, specifically, in the backscattered mode (d) it is more clearly visible than in Fig. 4c).

Sn62, Sn63 and Sn96 solder with optimized laser parameters are shown in Fig. 4a, b, c. Generally, good wetting of the leads and the PCB pad was found. No intermetallic layers at the solder interface to the copper pads could be detected by SEM at magnifications up to 5000 times. The structure of the Sn62 specimen (Fig. 4a) shows lead-rich primary dendrites. No intermetallics are visible. For Sn63 (Fig. 4b) the dendrites are fewer than for Sn62. A globular eutectic structure appears. Infra red-reflow soldering (Fig. 5a) shows, in comparison, a more equilibrium-like state with a fine-grained globular structure without dendrites. The structure of Sn96 (Fig. 4c) is shown at higher magnification in Fig. 5c and d. A microprobe analysis of the dendrites (dark areas of Fig. 5c) yielded a higher than average concentration of tin. A large number of micropores with diameters $< 2\ \mu m$ appear.

3.3. Thermal-induced strain cycles

For the assessment of the reliability of laser-soldered joints a thermal-cycling test according to ESA PSS-01-704 was performed. The temperature was cycled between -100 and $+100\,^{\circ}C$ with hold times of 30 min at the temperature extremes and heating/cooling rates of $10\,^{\circ}C\,min^{-1}$. The solder junctions were inspected after 10 and 100 cycles at their cross-sections and, in addition, after 100 cycles by shear tests.

For all cycled samples neither an optical degradation of the solder fillets nor failures visible in the metallographical inspection (such as hair-like cracks, fatigue cracks, deformations or detachment of soldered pads) were found. The cross-sections after thermal cycling (100 cycles) are given in Fig. 4d, e and f, for Sn62, Sn63 and Sn96, respectively.

TABLE II Shear strength (MPa)

Solder type	Uncycled	100 cycles	IR-reflow uncycled
Sn62	62.6	68.2	
Sn63	54.5	62.7	60.0 Cu-lead 30.2 Kovar lead
Sn96	54.5	60.0	

The globular microstructure of the Sn62 solder is not affected by thermal cycling. Some dendrites of the lead-rich phase are found in the uncycled (Fig. 4a) and cycled samples (Fig. 4d). Thus, this dendritic structure is not dissolved by secondary recrystallization effects during this thermal-fatigue test.

As with the Sn62 solder, no fatigue effects are found in the microstructure of Sn63 after thermal cycling. In both the cycled and uncycled sample a globular eutectic structure is observed (Fig. 4b, e). The crystallite sizes of the tin-rich and lead-rich phases are not affected by thermal cycling.

For the Sn96 solder, the dendritic microstructure is mainly preserved after ten thermal cycles. After 100 cycles the dendrites are dissolved to a large extent and only small residual crystallites are found (Figs 4f and 5b). The deformation of the solder can be followed in the microstructure of Fig. 4f. The residual crystallites are partly located along rows in the directions of high shear deformation. Despite this deformation, no macroscopic changes (like folding of the fillet surfaces) are present.

3.4. Shear strength

For the measurement of the shear strength, the samples were prepared in a way that one pair of soldered leads of the SO16 socket lying opposite was cut out. Then two pieces of PCB, each carrying one solder pad, were soldered to the described part of the SO16 component. In this way one pair of joints were tested and the strength of the weaker joint was measured. The shear strength of the joints soldered with optimized laser parameters was evaluated for dependence on the solder type and the number of thermal cycles. The values of shear strength are listed in Table II. The silver content improves the strength of the Sn62 solder with respect to Sn63. No degradation of the joint strength was found for the cycled samples. This is in accordance with the metallographic evaluation of the joints, where no change of the microstructure due to thermal cycling was observed.

4. Conclusion

The quality of a solder joint is highly dependent on the temperature course during soldering. Very high cooling rates due to heat dissipation into the component and the base material, both of which remain cool during the short irradiation times, lead to a very fine grained solder structure. Very thin intermetallic layers are formed at the solder/copper interfaces according to the short time heat affect.

The microstructures of laser-soldered joints of the types described in this paper were not changed by thermal treatment in a way which is important for practical use of the components. No cracks of any kind were introduced nor were detachments formed. Shear strength measurements did not show any degradation. Thus, laser soldering appears to be a unique soldering technique for high-reliability applications.

References

1. H. MIURA, *Electron Manuf.* **34** (1988) 43.
2. W. MÖLLER, D. KNÖDLER and K. V. VAYHINGER, *Optoelektronik Magazin*, **4**(8) (1988) 684.
3. N. SUENAGE, M. NAKAZONO and H. TSUCHIYA, *Welding Int.* **3** (1988) 269.
4. C. B. MILLER Jr, *Hybrid Circuit Technol.* **5** (1988) 27.
5. D. R. HALL, D. G. WHITEHEAD and A. POLIJANCZUK, Proc. 4th Int. Conf. on Lasers in Manufacturing, I.F.S., Birmingham, May 1987, p. 133.
6. L. MUSIEJOVSKY, "Optimization of process parameters for laser soldering of surface mounted devices", Masters Thesis, Technical University of Budapest, Hungary, (1990).

Received 27 April 1992
and accepted 19 January 1993